EEET ECOLOGICAL ENGINEERING & ENVIRONMENTAL TECHNOLOGY

Ecological Engineering & Environmental Technology, 25(12), 371–386
https://doi.org/10.12912/27197050/194949
ISSN 2299–8993, License CC-BY 4.0

Received: 2024.09.27
Accepted: 2024.10.28
Published: 2024.11.01

Combining Effluent Treatment Methods to Remove Ammonia Nitrogen from Tannery Wastewater

Edwar Aguilar-Ascón[1*], Liliana Marrufo-Saldaña[2], Julio Alexis Barra-Hinojosa[2]

[1] Universidad de Lima, Instituto de Investigación Científica, Grupo de Investigación en Tecnologías Exponenciales, Estudios Generales, Av. Javier Prado Este 4600, Surco, Lima, Perú

[2] Centro de Innovación Productiva y Transferencia Tecnológica del Cuero, Calzado e Industrias Conexas (CITEccal Lima). Instituto Tecnológico de la Producción (ITP), Caquetá Ave. 1300, 15094, Lima, Perú

* Corresponding autor's e-mail: eaguilaa@ulima.edu.pe

ABSTRACT

This study assessed the removal efficiency of ammonia nitrogen from tannery wastewater by combining electrocoagulation, ozonation, and ion exchange technologies. For this purpose, an electrocoagulation reactor equipped with aluminum electrodes, an ozonation tank, and a filtration system with zeolite were employed. The electrocoagulation treatment applied the response surface methodology with a 3^k factorial design with the following two factors: current intensity (I) ranging from 3 to 7A, and treatment time (t) from 10 to 30 min; the removal percentage of total suspended solids (TSS) is set as a response variable. Results indicate that the treatment time and current intensity were significant for the removal of total suspended solids TSS, at a confidence level of $p < 0,05$. Under these conditions, a TSS, removal efficiency of 98% was achieved. Through the electrocoagulation process, the chemical oxygen demand (COD) was reduced by 58%, while in the ozonation tank, an additional 23% of COD was removed. The filtration stage demonstrated that 13X HP zeolite can exchange ions with the ammonia nitrogen from tannery wastewater, wherein a 39% removal efficiency is reached at equilibrium. Thus, the integration of various treatment methods is a viable alternative to reduce wastewater from the tannery industry. The novelty of this research lies in the integration of three methods for treating tannery wastewater. The results show that the combination of these treatments provides a more effective solution for removing the pollutant load, especially nitrogen, compared to the use of individual treatment methods alone. The study opens new perspectives for optimizing multi-stage treatment processes.

Keywords: ammonia nitrogen, tannery, ozonation, response surface, aluminum electrodes.

INTRODUCTION

In Peru, many tanneries mix their effluents into one container or pond due to insufficient storage or treatment facilities, exacerbating compliance challenges with environmental discharge standards. Treating the effluents from this industry is a complex process due to the unitary stages that skins in the tanning process undergo, each carrying a distinct pollutant load due to the different chemical products applied to obtain a desired outcome. Among these pollutants, ammonia nitrogen is particularly difficult to remove through conventional treatment systems. Ammonia nitrogen in the tanning process originates from the use of ammonia salts during dehairing operations (Kong, et al., 2020), as well as from collagen degradation, which, upon hydrolysis, yields proteins, peptides, and amino acids (Leta, et al., 2005; Zhao, et al., 2019). The effects of ammonia nitrogen on aquatic ecosystems include eutrophication, posing toxicity risks to aquatic organisms (Leta, et al., 2005). The treatments applied for the removal of ammonia include chemical nitrogen removal (catalytic oxidation, electrolysis, ion exchange, ozone oxidation), physical removal (chemical precipitation, emulsion liquid membrane emulsion techniques), and biological

nitrogen removal (styrene butadiene rubber (SBR) membranes, biological membrane treatments) (Zhao, et al., 2019).

Previous studies have confirmed the high efficiency of electrocoagulation in removing chromium, achieving removal percentages of 99% for chromium, 56.8% for chemical oxygen demand (COD), and 69.2% for biochemical oxygen demand (BOD) (Aguilar, et al., 2019; Aguilar, et al., 2020; Deveci, et al., 2019). However, it has been established that the removal of ammonia nitrogen is insufficient, requiring the integration of electrocoagulation with other technologies to enhance treatment effectiveness. Hence, other technologies, such as ozonation and ion exchange, must also be integrated to fully treat these effluents. There are several precedents where at least two processes outlined in this study are combined for the treatment of several types of effluents.

The application of combined treatment processes has shown better removal results. One of these studies was conducted by (Barzegara, et al., 2019). Here, the authors used the electrocoagulation/ozonation process for treating greywater. Results revealed an 85% removal efficiency for (COD) and a 70% removal efficiency for total organic carbon. The combination of the electrocoagulation and ozonation methods generated a synergistic process that improves (COD) reduction times. In fact, the integrated process reduced (COD) by 88% in just 12 minutes. Furthermore, (Aziz, et al., 2016) proved that 100% removal of color and (COD) could be achieved through the ozonation–electrocoagulation process. Another study conducted by (Behin, et al., 2015) applied ozone-assisted electrocoagulation as an advanced oxidation process for the removal of acid triazo dyes. Under optimal conditions, the synergistic effect of the combined process achieved complete discoloration in 30 min with an energy consumption of 7.4 kWh⁄kg of dye removed. (Asaithambi, et al., 2016) also compared the effectiveness of the ozonation, electrocoagulation, and ozone-assisted electrocoagulation processes, where the hybrid electrocoagulation process was able to remove 100% of the color and 95% of the (COD).

Alternatively, other studies have also combined electrocoagulation with ion exchange using zeolite as a medium. One such study was conducted by (Vukojevi´c Medvidovi´c, et al., 2022), who integrated electrocoagulation and natural zeolite in the treatment of leachate from biological waste, achieving a (COD) removal of 99.34%, a TNK removal of up to 100%, and a turbidity removal of up to 99.82%. (Ham, et al., 2018) studied the removal of ammonia by activating synthetic zeolite in the aqueous phase through ion exchange in a batch. Among the adsorbents examined, modified synthetic zeolite A-4 was the most effective for removing ammonia. The optimal activation condition of zeolite A-4 was established through thermal treatment with Na^+ at 300 °C and a pH between 6 and 7. Another study by (Pan, et al., 2019) aimed to modify Chinese natural zeolite with NaCl and study its suitability as a low-cost clay adsorbent for removing ammonia from an aqueous solution. The results indicated that pH substantially affects ammonia removal, and maximum adsorption occurred at pH=8. (Ouyang, et al., 2021) applied faujasite zeolite in the adsorption of ammonia, among the zeolites tested, 13X-HP exhibited a great adsorption capacity, characterized by its small granule size of crystalline microspheres and its rough surface.

During electrocoagulation, metal cations are formed through the oxidation reaction of metallic anodes when subjected to the applied electric field. At the same time, the hydrogen gas bubbles produced at the cathode allow the flotation of contaminants to the surface. However, studies suggest that iron electrodes are unsuitable for treating tannery wastewater because they generate a black-colored effluent. According to (Ehsan Jafari, et al., 2023), aluminum undergoes oxidative dissolution in aqueous solution during the anodic process, as depicted in reaction (1). Furthermore, at the cathode, water undergoes reducing dissociation, as shown in reaction (2)

$$Anode: Al_{(s)} \rightarrow Al^{3+}_{(aq)} + 3e^- \quad (1)$$

$$Cathode: 2H_2O + 2e^- \rightarrow H_{2(g)} + 2OH^-_{(aq)} \quad (2)$$

At the cathode, the following reactions occur: (1) the production of abundant hydroxyl ions OH- that react in solution with aluminum cations to form coagulants; (2) the production of hydrogen gas H_2, which contributes to the destabilization of colloidal particles, leading to flocculation; and (3) the flotation of contaminants by adhering to the tiny bubbles formed by hydrogen evolution (electroflotation) (Ehsan Jafari, et al., 2023; Howe, et al., 2012). The aluminum ions Al^{3+} produced by the electrolytic dissolution of the anode act as a coagulating reagent, undergo hydrolysis, and form mononuclear complexes, as depicted in the following reactions (Ehsan Jafari, et al., 2023; Burns, et al., 1997):

$$Al^{3+} + H_2O \rightarrow AlOH^{2+} + H^+ \quad (3)$$

$$AlOH^{2+} + H_2O \rightarrow Al(OH)_2^+ + H^+ \quad (4)$$

$$Al(OH)_2^+ + H_2O \rightarrow Al(OH)_3 + H^+ \quad (5)$$

$$Al(OH)_3 + H_2O \rightarrow Al(OH)_4^- + H^+ \quad (6)$$

Ozone is a strong oxidant that can react in aqueous solution with several organic and inorganic compounds either through direct ozone attack and/or through an indirect reaction of free radicals involving the hydroxyl radical induced by ozone decomposition in water (Asaithambi, et al., 2012). One of the ways to generate ozone for water treatment is by subjecting oxygen (O_2) at a high electrical charge, causing molecules to separate, and thereby forming ozone (O_3). This ozone gas is then added to water through diffusers to degrade organic matter, in addition to presenting a high disinfectant power (Preethi, et al., 2009)

Similarly, ion exchange process is defined as an external surface complexation, involving the substitution of cations in the structure of exchangeable solids. Among the most researched ion exchange materials for ammonia removal, zeolites are notable for their high efficiency and low costs. (Sundhararasu, et al., 2022; Chung, et al., 2000; Khamidun, et al., 2022). it has been systematically studied for its potential application in effluent treatment due to its large specific surface area, compared to other adsorbents, and high ion exchange capacity. (Kamimoto, et al., 2020). Zeolites are three-dimensional structures of tetrahedral aluminosilicates formed by the union of TO_4 tetrahedra, or basic construction units, where T represents silicon and/or aluminum atoms in which aluminum and silicon atoms are bonded through covalent bonds to common oxygen atoms to form cages and interconnected channels (Huang, et al., 2018). The valence difference between silicon (+4) and aluminum (+3) results in an excess of negative charge in the crystalline structure. (De Magalhães, et al., 2022). They are characterized by their ion exchange and adsorption properties, due to their porous nature and their content of alkaline or alkaline earth cations fixed to their cavities that can be easily exchanged with surrounding positive ions. The exchange process involves intra-particle diffusion in the pores (Wen, et al., 2006; Zheng, et al., 2008, Ibrahim, et al., 2017, Pan, et al., 2022).

Natural zeolites exhibit a porous structure and comprised hydrated aluminosilicate minerals, possessing valuable physicochemical attributes including cation exchanges, molecular sieving, catalysis, and sorption (Wang, et al., 2010). The study of natural and synthetic zeolites for the exchange of ammonia ions from aqueous solutions has been undertaken by different researchers (Probst, et al., 2022). Within the zeolite structure, alkali or alkaline earth cations are reversibly bound within the cavities via weak electrostatic bonds and can readily be exchanged by adjacent positive ions such as N_a^+, K^+, Ca^{2+}, Mg^{2+} thereby enhancing their mobility and exchange capacity with solution cations. This property renders zeolite capable of effectively removing heavy metals as well as ammonia ions (Ibrahim, et al., 2017). The application of ion exchange for contaminant removal can be carried out in batch or using fixed bed. In the latter, the adsorbate flows through the adsorbent contained in a column. The importance of this method lies in its feasibility for scaling up. (Sundhararasu, et al., 2022). Many of the studies conducted in fixed beds reported using synthetic ammonia samples to assess the ion exchange capacity of different types of zeolites (Sundhararasu, et al., 2022; Thushari, et al., 2016; Măicăneanu, et al., 2011).

Therefore, electrocoagulation has shown optimal removal of BOD, COD, chromium, among other pollutants in previous studies, but ammonia has been found to be difficult to remove. Thus, the present study evaluated the treatment of an effluent sample from a tannery pilot plant. The treatment consisted of three stages: electrocoagulation, ozonation and ion exchange. Electrocoagulation and ozonation are intended to remove the pollutant load related to organic material and metals, and these results are analyzed using response surface methodology. Ion exchange aims to complement the treatment by removing ammonia to levels required by environmental standards.

The objective of this research is to evaluate the effectiveness of electrocoagulation, ozonation, and ion exchange in the removal of ammonia nitrogen from tannery effluents. The novelty of this research lies in the integration of three technologies for the treatment of tannery wastewater.

MATERIALS AND METHODS

Tannery wastewater

The tannery wastewater was provided by the Center for Productive Innovation and

Technological Transfer of Leather, Footwear and Related Industries (CITEccal), which was obtained from the processing of cow hides at its tanning pilot plant. The sample was a composite effluent and was prepared by mixing the effluents collected at the end of the stages of soaking, unhairing, bating, deliming, washing, pickling and tanning of the tanning process, where different tanning salts, reagents and substances are applied.

Obtention of zeolite sample

In this research, zeolite 13X-HP was used due to its availability in the local market. Zeolite 13X-HP belongs to the faujasite (FAU) family of zeolites, with a pore diameter ranging from 0.74 to 1.12 nm. This structure allows for a high adsorption capacity due to its large pores, which facilitate the adsorption of larger molecules and a greater amount of adsorbate. In contrast, zeolites of type A have a pore diameter of approximately 0.4 nm. Although these are effective for the adsorption of small ions, their smaller pores may limit the adsorption capacity for ammonium nitrogen compared to zeolites 13X-HP. (Ouyang et al., 2021). The zeolite was characterized using Fourier transform infrared spectroscopy (FTIR) with a SHIMADZU QATR 10 spectrophotometer 10, through Attenuated Total Reflectance (ATR) in the range of 4000–650 cm^{-1}.

Integrated electrocoagulation–ozonation–Ion exchange system

The integrated treatment system addressed the sequential treatment of the tannery wastewater sample using three treatment methods. It began with the electrocoagulation process, followed by the application of the ozonation process, and concluded with ion-exchange through a fixed-bed system. The details of each stage of the treatment are described below.

The electrocoagulation reactor is designed with dimensions of 16×16×22 cm^3 (length × width × height). Eight aluminum electrodes were installed, functioning as anodes and cathodes, with an area of 100 cm^2. A power source capable of supplying a current intensity of up to 50 A was used. For the ozonation of the treated water, a contact tank equipped with perforated hose diffusers for ozone supply, generated by an ozonator with the capacity to supply ozone concentrations of up to 15 g/h, was used (Fig. 1).

For the ion exchange system, a fixed-bed adsorption system was designed and assembled. This involved acquiring a peristaltic Vikye brand pump, 6 mm silicone tubes, 3/4" PVC tubes of different lengths (which varied from 5 to 15 cm), 3/4" PVC unions, 3/4" PVC universal thread unions, 3/4" PVC female caps, and a 6 mm flow regulator. Adsorption columns were assembled by connecting PVC tubes with the cap, which had 5 holes of ~ 1 mm diameter each arranged in a cross shape. Additionally, 0.3 g of cotton was placed between the cap and the tube's outlet to homogenize effluent flow. The flow rate of the system was regulated using an electronic universal key and flow regulator and stablished at 14.5 ml/min according to previous studies and system tests. The effluent was pumped from a feeding tank to the fixed-bed column, and the treated effluent was collected in a reception tank for analysis. The synthetic zeolite used originated from 13X - HP, with an

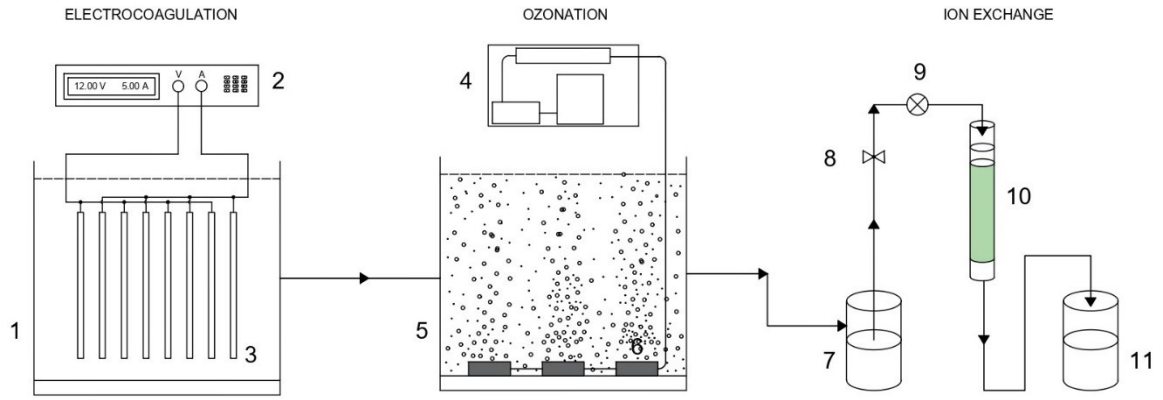

Figure 1. The integrated treatment system: (1) electrocoagulation reactor, (2) power source, (3) aluminum electrodes, (4) ozonizer, (5) ozonation tank, (6) diffusers, (7) feed tank, (8) flow regulator, (9) peristaltic pump, (10) fixed bed column with zeolite, (11) reception tank

effective pore diameter of 10 A° (1 mm) and a particle size of 1.6–2.5 mm used as an air purifier minly in the production of medical oxygen with pressure swing adsorption technology.

Experimental procedure

In the first stage, the tannery wastewater was treated using the electrocoagulation reactor with aluminum electrodes, applying a response surface methodology. The variables considered were current intensity and time, with the percentage of total suspended solids TSS removal as the response variable. In the second stage, the water treated by electrocoagulation underwent treatment in an ozonation tank, to which ozone was supplied using an ozone generator prototype at concentrations of 7 and 15 g/h. In order to evaluate the impact of contact time between ozone and the compounds present in the water, three contact intervals were selected: 30, 60, and 90 minutes. This is because contact time significantly influences advanced oxidation processes. According to previous studies, it has been observed that with a contact time of up to 30 minutes, only a 50% efficiency in contaminant removal is achieved (Aguilar, et al., 2023). On the other hand, research by (Lanzetta, et al., 2023) and (Prabhakaran, et al., 2022) indicates that after 45 minutes of ozonization, significant reductions in COD can be achieved, with removal efficiencies ranging from 31% to 51%. Oxygen will be obtained by pumping natural air into the ozone generation chamber. The water resulting from the two previous processes will undergo ion exchange using a column packed with zeolite, where the percentage of ammonia nitrogen removal will be assessed.

For pH, conductivity, and temperature measurements, the Oakton PCS 35 multiparameter device will be used. To quantify TSSs (response variable), a portable colorimeter DR900 Hach was used. The percentage of removal of TSS and ammonia nitrogen is determined by Equation 7

$$Y_n = \%R = \left(\frac{C_i - C_f}{C_i}\right) \times 100 \qquad (7)$$

where: %R – removal percentage, C_i – initial concentration, C_f – final concentration

To determine the influence of column height on the percentage removal of NH_4^+, heights of 5 and 15 cm were evaluated with zeolite masses of 12.65 and 37.8 g, respectively, at a flow rate between 17 and 18 ml/min, using the effluent under study. Once the height with the highest removal efficiency was established, and in order to study the adsorption capacity of the zeolite, the effluent was passed through the column, and samples of the eluate were taken over a time range from 15 to 40 minutes at intervals of 5 minutes. In this experiment, the flow rate was adjusted to 14.5 ml. The effluent used corresponded to the composite effluent previously treated by electrocoagulation and ozonation. (Fig. 1) presents a diagram of the fixed-bed adsorption system used. The samples of the effluent eluted from the column were sent to an accredited laboratory for testing to determine their ammonia nitrogen content. Likewise, a sample of the effluent before treatment with the zeolite was also sent. The method used for the ammonia nitrogen analysis was SMEWW-APHA-AWWA-WEF Part 4500-NH3 D, 24th Ed. 2023.

Experimental design using response surface methodology

For this study, the response surface methodology was used, which allows optimizing the operating parameters of the electrocoagulation process with the fewest number of experiments. (Ebba, et al., 2022; Wu, et al., 2021). The specific method initially considered for optimization was changed because only 2 factors and 3 levels were considered in the experimental design based on preliminary results. To obtain the optimal values for electrocoagulation treatment, the response surface methodology was applied using a full 3^k factorial design, with two factors, electric current intensity (x_1) and treatment time (x_2), and three levels (-1, 0, +1) (see Table 1). Nine experiments with nine replicates and two central points were conducted. The response surface methodology involves mathematical techniques

Table 1. Independent variable ranges and their levels

Factor	Variable	Levels		
		−1	0	+1
x_1	Intensity (A)	3	5	7
x_2	Time (min)	10	20	30

applied to the improvement and optimization of complex systems (Choi, et al., 2020). This method is used to assess the effects of different parameters and their interactions on the responses from the system (Choi, et al., 2020; Xu, et al., 2015). Equation 8 denotes the second-order polynomial equation used in (RMS), which evaluates each of the independent variables at its three levels.

$$Y = \alpha_0 + \sum_{i=1}^{3} \alpha_i X_i + \sum_{i=1}^{3} \alpha_{ii} X_i^2 + \sum_{i=1}^{3} 1 \sum_{j=i+1}^{3} \alpha_{ij} X_i X_j \quad (8)$$

where: Y is the response value, a_0 is the constant intercept term, a_i is the linear term, a_{ii} is the squared quadratic term, a_{ij} is the regression coefficient of the interaction term, and X_i and X_j are independent variables. The independent parameters were set as electric current intensity x_1 and treatment time x_2, and the percentage of TSS removal was defined as a response variable. (See Table 1). For evaluation and statistical analysis, the Design Expert 11.1 software will be used, providing an ANOVA table at a confidence level of 95%. The fit of the polynomial model will be determined using the coefficient of determination R_2 and R_{adj}.

Zeolite fixed bed ion exchange treatment

While carrying out adsorption and ion exchange fixed bed treatment processes, the breakthrough curves predict the bed lifespan and regeneration time in the ion exchange system. The breakthrough capacity is the point at which the outlet concentration reaches an upper limit, which is a percentage (usually 5 % to 10%) of the inlet concentration (Thushari, et al., 2016). The maximum adsorption capacity q_{total} (mg) in the column is determined by the Equation 9–10, integrating the concentration of adsorbed ammonia as a function of time "t" [30].

$$q_{total} = \frac{Q}{1000} \int_{t=0}^{t=total} C_{ad} dt \quad (9)$$

$$C_{ad} = C - C_i \quad (10)$$

where: C represents the concentration of ammonia eluted at different times, expressed in mg/L, C_i is the initial untreated sample concentration, expressed in mg/L, Q is the flow (mL⁄min).

$$C_{ad} = C - C_i \quad (11)$$

Equilibrium capacity (q_e) was determined by dividing the maximum adsorption capacity q_{total} (mg) in the column by the dry mass of the adsorbent. The system removal efficiency was calculated according to the Equation 11. Different mathematical models are used to explain the behavior of the system with the aim of scaling it up. Among them, the Thomas mathematical model stands out, which assumes Langmuir adsorption–desorption kinetics and second-order reversible reaction kinetics. Equation 12 describes the linearized form of the model:

$$\ln\left(\frac{C_i}{C} - 1\right) = \frac{k_1 q_0 M}{Q} - \frac{k_1 C_i V}{Q} \quad (12)$$

where: C is the concentration of ammonia eluted at different times expressed in mg/L, C_i is the initial concentration of the untreated sample expressed in mg/L, Q is the flow rate (L⁄min), k_1 is the rate constant expressed in L⁄mg, M is the zeolite mass in g, and q_0 is the maximum exchange capacity of the zeolite.

RESULTS AND DISCUSSION

Characterization of the tannery effluent

The results of the characterization of the sample are reported in (Table 2), where they are compared with the Peruvian environmental standards for wastewater discharges in the sewage system or maximum permissible values (VMAs).

Electrocoagulation treatment process

Results from the response surface methodology

Table 3 illustrates the 3^k factorial response surface design, incorporating the current intensity x_1

Table 2. Physicochemical analysis of the effluent

Parameters	Value
Total suspended solids (mg/l)	938
Chemical oxygen demand (mg/l)	3758.5
Biochemical oxygen demand (mg/l)	1556.7
Ammonia nitrogen (mg/l)	266,681
Turbidity (NTU)	1134
pH	7.98
Conductivity (µS/cm)	13870
Chromium (mg/l)	100,384
Hexavalent chromium (mg/l)	<0,010
Oils and fats (mg/l)	17.50
Fecal coliforms (MPN/100 ml)	<1.8
Sulfides (mg/l)	19,965

Table 3. Experimental design

Run	Block	Levels		Current Intensity (A)	Time (min)	TSS Removal (%)	
				x_1	x_2	Experimental	Predicted
1	1	−1	−1	3	10	83	83.25
2	1	0	−1	5	10	90	89.75
3	1	1	−1	7	10	93	93.47
4	1	−1	0	3	20	92	92.12
5	1	0	0	5	20	94	93.78
6	1	1	0	7	20	96	96.88
7	1	−1	1	3	30	94	94.51
8	1	0	1	5	30	95	95.19
9	1	1	1	7	30	96	95.89
10	1	0	0	5	20	97	98.45
11	2	−1	−1	3	10	83	83.25
12	2	0	−1	5	10	92	91.12
13	2	1	−1	7	10	94	94.58
14	2	−1	0	3	20	90	89.76
15	2	0	0	5	20	93	93.45
16	2	1	0	7	20	95	94.89
17	2	−1	1	3	30	93	92.99
18	2	0	1	5	30	95	95.13
19	2	1	1	7	30	96	96.60
20	2	0	0	5	20	98	97.89

and treatment time x_2 factors, each with three levels and 20 experiments. Through Multiple Regression analysis, the response (y) was correlated with the design factors x_1, x_2 using the second-order polynomial (see Table 4). The quadratic regression model for TSS removal (y)(y), in terms of the coded factors, is is reported in (Tables 3 and 4).

To assess significant variables, the P and F values of the ANOVA of the response variable are shown in (Table 5) below. The results indicate that current intensity x_1 and treatment time x_2 had a significant impact at a confidence level of 95% ($p < 0.05$) on TSS removal. An F model with a value of 23.72 and a Probability > F of less than 0.0001 imply that this model is significant. Furthermore, R^2 values close to 1 demonstrate satisfactory agreement between the results obtained and predicted (Sefatjoo, et al., 2020). Figure 2 displays the three-dimensional and two-dimensional response surface plots, based on two independent factors, to understand their main interaction effects (Dil, et al., 2019).

Table 4. Statistical parameters obtained by RMS (%)

Source	Sum of Square	df	Mean Square	F-value	p-value
Block	0.0500	1	0.0500		
Model	272.97	5	54.59	23.72	< 0.0001
x_1: Current intensity (A)	102.08	1	102.08	44.35	<0.0001
x_2: Time (min)	96.33	1	96.33	41.85	< 0.0001
x_1x_2	32.00	1	32.00	13.90	0.0025
x_1^2	15.48	1	15.48	6.73	0.0223
x_2^2	20.02	1	20.02	8.70	0.0113
Residual	29.93	13	2.30		
Lack of fit	12.93	11	1.18	0.1382	0.9901
Pure error	17.00	2	8.50		
Cor total	302.95	19			
R^2 = 90.12%; R^2_{adj} = 86.32					

Table 5. Analysis of variance (ANOVA) for the RSM quadratic model

Answer	R^2	$Adj - R^2$	p	Quadratic response model based on least squares
	%			
TSS removal (%)	90.12	86.32	< 0.0001	$y = 52.65774 + 8.01190x_1 + 1.61190x_2 - 0.1x_1x_2 - 0.455357x_1^2 - 0.20714x_2^2$
TSS removal (%); y, current intensity (A); x_1 time (min); x_2				

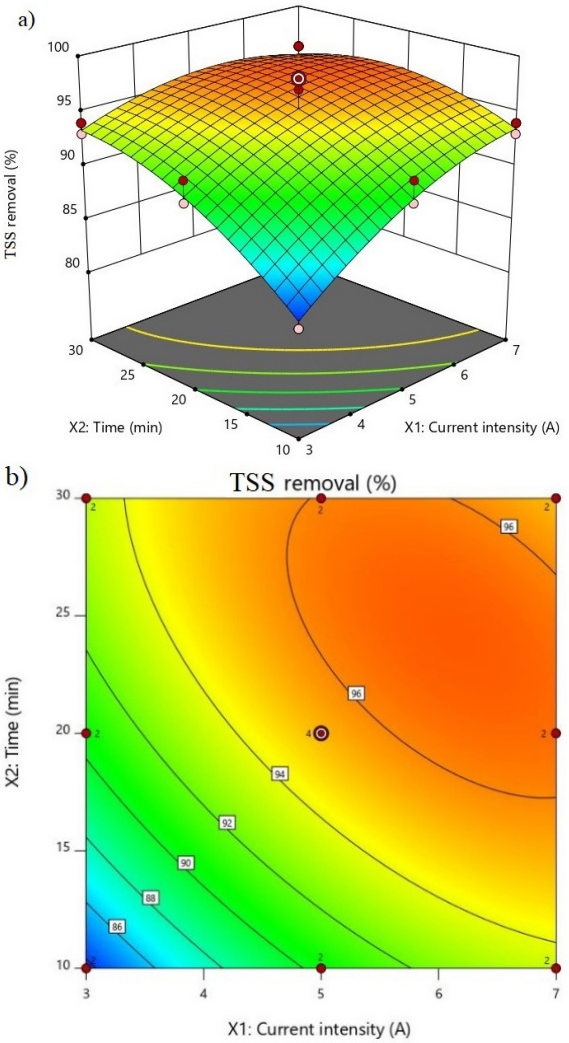

Figure 2. Three-dimensional (3D) and two-dimensional (2D) response surface Plots for TSS percentage removal

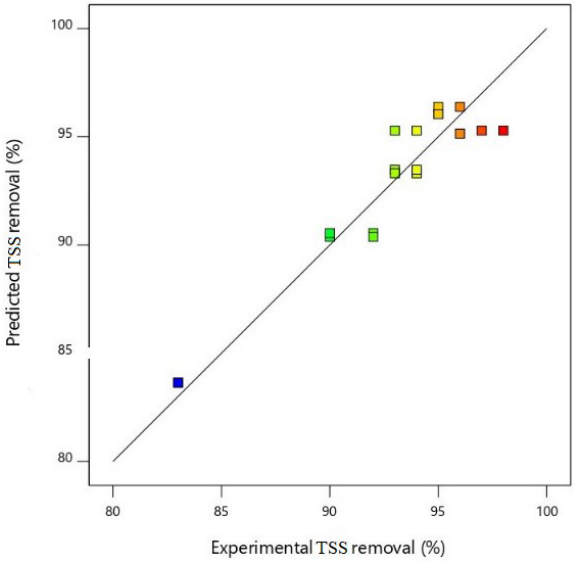

Figure 3. Regression chart illustrating the correlation between experimental data and predicted values obtained through response surface methodology, describing the percentage of total suspended solids removal

In Figure 3, it can be observed that the predictive model used is quite accurate in estimating the removal of TSS, as it falls within the range of 80-100%. Although small deviations are observed, they are mostly within an acceptable range. This is measured by the correlation index, which in this case is $R^2 = 0.9012$ (90.12%), indicating a good relationship between the experimental data and the expected data. The variables current intensity and time were optimized using RSM to achieve maximum TSS removal efficiency. The optimal values found for current intensity and time were 5 amperes and 20 minutes, resulting in a maximum TSS removal percentage of 98% (18.76 mg/L remaining).

Effects from current intensity on TSS Removal TSS

Current intensity is a critical parameter in electrocoagulation, as it influences the rate of bubble generation, coagulant dosage rate, size, and development of flocs, all of which impact the effectiveness of electrocoagulation (Sriram, et al., 2023; Zaied, et al., 2020). Anode dissolution rate rises with increasing current density, resulting in more metal hydroxide flocs, thereby enhancing pollution removal efficiency. However, exceeding the optimal current density does not affect contaminant removal efficiency, but escalates treatment costs (Sriram, et al., 2023). In this study, three current intensity values of 3, 5 and 7 amperes were employed. In Figure 2, it is observed that the current intensity shows an optimal behavior around 5 amperes. Current intensities lower than this value seem to be insufficient

to achieve efficient removal, while higher intensities do not significantly increase TSS removal and could lead to increased energy consumption. On the other hand, TSS removal efficiency rapidly increases from 83% to 98% as current intensity increases from 3 to 7 amperes, respectively. This is attributed to the increase in Al^{3+} and, consequently $Al(OH)_3$ particles released by the anode as the current intensity increases (Deveci, et al., 2019). These results are consistent with those reported by (Aboulhassan, et al., 2018), who reports an efficiency of 96%. Furthermore, (Leta, et al., 2005), reports efficiencies of 99%, while (Varank, et al., 2014) achieve 85% TSS removal efficiencies.

Effects from treatment time on TSS removal

In electrocoagulation, the effectiveness of contaminant removal depends on the duration of the electrolysis process. As electrolysis time increases, contaminant removal efficiency also increases, as evidenced in this study concerning TSS removal. However, once the optimal electrolysis time is reached, contaminant removal efficiency remains constant, showing no further improvement as electrolysis times increase. The dissolution of the anode produces metal hydroxides. With longer electrolysis durations and constant current density, the production of metal hydroxides also increases. (Sriram, et al., 2023; Abdulrazzaq, et al., 2021). According to Faraday's Law, the length of the electrolysis process during the electrocoagulation process affects the rate of release of metal ions into the system. (Malakootian, et al., 2010).

TSS removal efficiency was assessed after 10, 20, and 30 min of treatment. Aluminum metal ions (coagulants) are produced through the dissolution of the anode when the current flows through the electrode. (Bishwatma, et al., 2022). The results of this parameter are depicted in (Table 3) and (Fig. 2), confirming that the efficiency of TSS removal increases with treatment duration. It is observed that when the treatment time increases from values close to 10 minutes to around 25 minutes, the TSS removal efficiency increases steadily. However, beyond 25 minutes, the gain in efficiency is minimal and even negative, suggesting that longer times do not result in any significant additional benefits and could lead to unnecessary energy consumption. It is observed that after 20 minutes and 3 amperes, the TSS (Total Suspended Solids) are reduced from a value of 938 to 89 mg/l, reaching an efficiency of 90%. Meanwhile, after 20 minutes and 5 amperes, the TSS are reduced to a value of 19 mg/l, achieving an efficiency of 98%. Moreover, it is noted that at the 30-min mark, the efficiency either remains constant or declines in some cases. These findings closely align with those of (Espinoza-Quiñones, et al., 2009) who reported an approximate efficiency of 73% removal of TSS. In addition, (Varank, et al., 2014) reported high efficiencies that approached 85% removal. Identifying the optimal treatment duration is crucial, as excessively prolonged periods can lead to high electrode and energy consumption (Can, et al., 2006).

Effect from ozone in the ozonation reactor

Research indicates that the ozonation of tannery effluents not only facilitates color removal, but also boosts the biodegradability index of the effluents (Preethi, et al., 2009; Houshyar, et al., 2012). In addition to pre- and post-ozonation, ozone can also be applied within biotreatment as an intermediate step with significant results. The effluent treated via electrocoagulation under optimal conditions underwent treatment in an ozonation tank to lower the COD concentration and enhance effluent quality before undergoing ion exchange with zeolite. The ozonation process was planned to be conducted in a separate tank to prevent microbubble formation from the electrocoagulation process, and to achieve better ozone distribution (Aguilar, et al., 2024). In the electrocoagulation reactor, a significant amount of COD concentration is removed, achieving an efficiency of 58% (1578.57 mg/L remaining). To reduce refractory COD, two ozone concentrations (7 and 9 g/h) and three contact times 30, 60, 90 minutes were applied. In Figure 4, the maximum

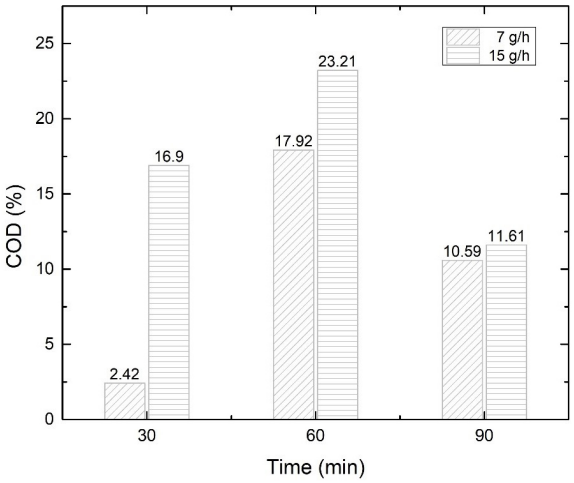

Figure 4. TSS removal percentage COD in the ozonation process

percentage of COD removal was 23% (1215.50 mg/L remaining), at a rate of 15 g/h, and a contact time of 60 minutes. This low performance may be due to the formation of refractory intermediate compounds during the electrochemical process (Manenti, et al., 2014). However, at a dose of 7 g/h and 30 min, the removal of COD is minimal. Similar findings are reported by (Srinivasan, et al., 2012), who used ozone in secondary treatment, obtaining of COD removal efficiencies ranging from 34.9% to 33.9% with pH values of 3 and 12, respectively. Additionally, at pH values close to 7, only a slight increase in COD was observed, which may be due to the generation of simpler organic compounds from larger molecular compounds. (Srinivasan, et al., 2012; Iaconi, et al., 2002).

Another study conducted by (Houshyar, et al., 2012), indicates that they achieved COD removal efficiencies of 60% in tannery wastewater using sodium hydroxide to reach an optimal pH of 9. Alternatively, (Dogruel, et al., 2004) states that the highest COD removal with ozone is obtained in the phase where organic matter is easily biodegradable, achieving efficiencies of 22% with a feed time of 5 minutes and an ozone flow rate of 42.8 mg/min.

Ion exchange treatement process

The tannery wastewater sample treated at the optimal conditions of electrocoagulation and ozonation was then subjected to ion exchange treatment.

FTIR analysis of zeolite

Figure 5 shows the FTIR spectrum of the zeolite used in the present investigation. The absorption band around 3332.77 cm^{-1} corresponds to the O-H stretching vibration of adsorbed water and/or hydroxyl groups (OH) present on the surface of the zeolite. This band indicates the presence of water and OH groups that may be attached to the active sites of the zeolite. The band at 1644.60 cm^{-1} is associated with the bending vibration of water adsorbed in the zeolite structure. This signal confirms the presence of water molecules in the pores of the zeolite. The band at 950.33 cm^{-1} corresponds to the asymmetric stretching of (Si-O) or (Al-O) bonds, which is characteristic of the tetrahedral units of silicon (SiO_4) and aluminum (AlO_4) that form the crystalline structure of the zeolite. The band at 752 cm^{-1} is attributed to the external asymmetric stretching of Si-O-Si bonds. This band is representative of the connectivity between silicon tetrahedra in the zeolite structure. The band at 672 cm^{-1} corresponds to the internal tetrahedral stretching, which also indicates the tetrahedral structure of Si-O and Al-O bonds in the aluminosilicate framework (Ouyang, et al., 2021 Kongnoo, et al., 2016; Wang, et al., 2020) (Fig. 5).

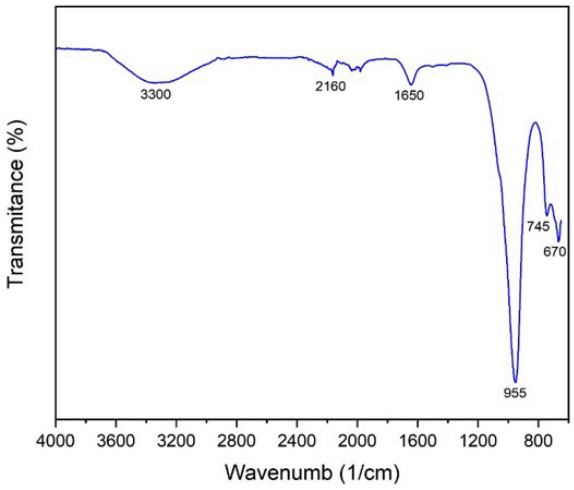

Figure 5. FTIR spectrum of the 13 X zeolite used in the treatment

Application of a fixed-bed treatment

The pH of the sample was found to be in the range of 6 to 7. In an aqueous solution, ammonia can exist in non-ionized form NH_3 and/or ionized form NH^{4+} depending on the pH and temperature. The ion exchange process with the adsorbent can only remove the ionized form (Fashi, et al., 2021). The exchange capacity remains constant up to a pH of 7. During the ion exchange process, alkaline or alkaline earth ions are replaced by NH^{4+} ions, leading to an increase in the concentration of the former in the liquid phase (Rahmani, et al., 2004). Several studies have reported that ion exchange increases as the particle size of zeolite decreases. For example, Wen reported in a batch study that particles ranging from 1.0 to 3.2 mm had better efficiency 72% for ammonia removal than particles of 8–15 mm. In this research work, the zeolite used had a diameter of 1.6–2.5 mm (Wen, et al., 2006).

The concentration of NH^{4+} determined in the untreated sample with zeolite was 341.2 mg/L. It should be noted that the concentration of ammonia did not decrease significantly with the electrocoagulation and ozonation treatments. Preliminary tests were carried out to evaluate de effect of the column height on NH^{4+} removal these were performed at 14.5 ml/min for 35 minutes (this treatment time was set as the necessary volume for

analysis was 0.5 L). The results from the column of 15 cm indicated a higher removal percentage of 29.96 %, while the removal percentage for the 5 cm column was 19.04 %. Thus, the higher the column, the greater the ammonia removal. This finding is consistent with the results of (Zheng, et al., 2008), who used column heights of 1.07, 21.4, and 38.5 cm for a synthetic ammonia solution of 80 mg/L, achieving removal percentages of 30.74%, 47.25%, and 55.56%, respectively. Because of these results, the column height of 15 cm was stablished for the following experiments.

Table 6 displays the ammonia concentrations measured in the eluates collected over time, along with the corresponding removal percentages. At 5 min of elution, a 78 % removal of ammonia is achieved; however, by 20 minutes, column saturation has been reached, removing only 39 % of ammonia. It has been reported that the removal efficiency of zeolites is influenced by various parameters such as contact time, initial ammonia concentration, adsorbent dosage, temperature, competing cations and anions, and dissolved organic matter (Huang, et al., 2018). Based on these results, there is a steady rise in NH_4^+ concentration in the eluate as time (t) progresses until t = 20 min. This trend suggests the occurrence of the adsorption process, as the ammonia concentration in the eluate increases with the passage of fluid through the adsorption system. Additionally, it is noted that the maximum adsorption capacity is likely to be reached around the 20-min mark.

When evaluating the upper breakthrough limit, where the eluate concentration equals 10% of the inlet flow concentration and is equal to 34.12 mg/L, we determined that breakthrough has occurred in the system because at 5 min of elution, the eluate concentration of 74.42 mg/L exceeds the breakthrough point. At 5 min of elution, a 78% removal of NH_4^+in the sample is achieved; however, by 20 minutes, column saturation has been reached, removing only 39% of NH_4^+ It has been reported that the removal efficiency of zeolites is influenced by various parameters such as contact time, initial ammonia concentration, adsorbent dosage, temperature, competing cations and anions, and dissolved organic matter (Huang, et al., 2018).

Among the cations and anions identified as competitors for exchange sites in zeolite, we find K^+, Na^+, Ca_2^+, Mg_2^+, Zn_2^+, Cd_2^+ Cl^-, $NO_3^-, SO4_2^-$ *and* $PO4_3^-$ (Huang, et al., 2018; Eberle, et al., 2023), with K^+ being the main competitor showing greater affinity for zeolite than NH_4^+ (Thushari, et al., 2016). It has been determined that the selectivity for Ion Exchange in clinoptilolite occurs in the following order: $K^+ > NH_4^+ > N_a^+ > C_a^{2+} > M_g^{2+}$ (Xuejun, et al., 2007). In the effluents of the tanning process, ions such as N_a^+ and C_a^+ are present, originating from chemical inputs used, such as sodium chloride, lime, sodium bicarbonate, and sodium formate. para el caso de esta muestra, estos no habrían sido removidos significativamente por los otros tratamientos y estarían compitiendo por los sitios de intercambio, disminuyendo la capacidad de intercambio.

Alternatively, lower flow rates lead to increased saturation time due to enhanced interaction between the adsorbent and the sample analytes. Some of the flow rates examined ranged from 3 to 20 ml/min. Given this context and the preliminary assessment, the system was fine-tuned to operate at a flow rate of 14.5 ml/min. Nevertheless, considering the results obtained and to enhance column removal efficiency, a comprehensive investigation into flow rates is recommended.

Upon assessing experimental data using Equations 7 and 8, a q_{total} of 102.15 mg and a q_e of 2.70 mg/g were derived. Similarly, applying the Thomas mathematical model yielded a rate constant K1 of 0.00014 L/min and a maximum

Table 6. Ammonia nitrogen results in the raw sample and samples treated at different elution times

Treatment	Time (min)	H_4^+ (mg/L) in the eluate (C)	E (%)
M1	5	74.42	78.19
M2	10	134.09	60.70
M3	15	172.65	49.40
M4	20	209.57	38.58
M5	25	202.41	40.68
M6	30	218.43	35.98
M7	35	202.29	40.71
M8	40	230.60	32.42

adsorption capacity of 2.64 mg/g. The experimental data exhibited a 75% fit to this model. (Fig. 6) illustrates a typical breakthrough curve.

Sundhararasu, et al., 2022 documented a maximum adsorption capacity at equilibrium ranging from 2.067 to 2.198 mg/g for a flow rate of 10 ml/min and a range between 1.346 and 2.200 mg/g for a flow rate of 20 ml/min when utilizing Na-Zeolite-Based Geopolymers for removing ammonia from a synthetic sample with a concentration of 40 mg/L. A study on the application of zeolites in NH_4^+ removal from a wastewater treatment plant reported values ranging between 2.21 and 2.24 mg/g for kt, varying from 0.0016 to 0.0062 L h^{-1} mg^{-1} for columns ranging from 2 to 15 cm, thereby achieving an 88.91% fit to the Thomas mathematical model (Khamidun, et al., 2020; Wijesinghe, et al., 2016) determined the maximum adsorption capacity for Australian natural zeolites and sodium-modified zeolites to be between 9.48 and 11.83 mg – N/g, respectively, for an initial NH_4^+ concentration between 10 and 1000 mg – N/L (Măicăneanu, et al., 2011) found capacities of 13.14821 and 11.8518 mg/g for volcanic zeolites with varying clinoptilolite content. As can be seen, the maximum adsorption capacity of the studied zeolite is very close to that determined by (Sundhararasu, et al., 2022).

To comply with the maximum permissible limit for NH_4^+ established in Executive Order No. 010-2023-MINAM, which is 10 mg/L, operating conditions must be adjusted, zeolite content must be modified, serial systems must be used, and/or supplementary adsorbents must be used.

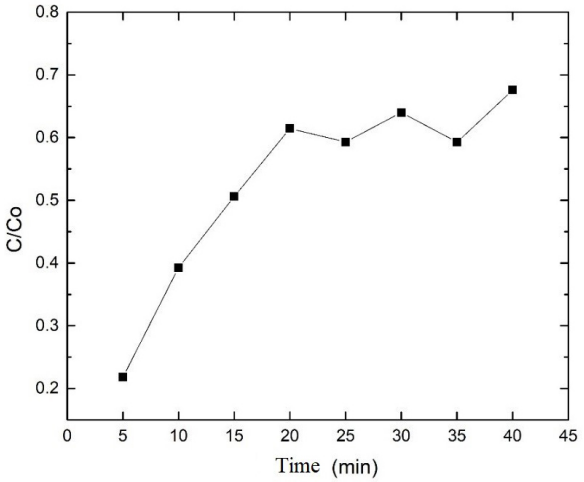

Figure 6. Effect from flow rates on the breakthrough curve for ammonia adsorption

CONCLUSIONS

This study confirms that an integrated system combining electrocoagulation and ozonation effectively removes TSS, COD, and ammonia nitrogen from tannery wastewater. The results from the initial electrocoagulation treatment stage highlight the significant impact of current intensity and treatment time on TSS removal, achieving removal efficiencies of 98%, and 58% for COD. During the ozonation stage, with a duration of 60 minutes and a rate of 15 g/h, COD was reduced by 23% and TSS by 20%. These results indicate the accomplishment of the VMAs for TSS and a close value for the COD.

In the subsequent stage, under specified treatment conditions, zeolite 13X HP was able to exchange ions with the ammonia nitrogen from tannery wastewater, reaching a removal efficiency of 39% at equilibrium, the resulting value still exceeds the VMA stablished for ammonia. Furthermore, the maximum adsorption capacity of the zeolite was determined to be 102.5 mg, with a maximum adsorption capacity of 2.70 mg/g, comparable to results obtained using the Thomas mathematical model. To enhance removal efficiency, adjustments to operating conditions such as column height and elution flow rates are necessary, along with considerations for establishing series processes, modifying zeolite structure, or complementing treatment with other adsorbents. Another crucial research subject is column regeneration and its associated costs when scaling up the technology. Even though the ammonia removal achieved by ion-exchange did not accomplished the environmental standard, this study reveals that combining these methods results in a more effective solution when compared with the individual treatments, providing more effective techniques for treating complex tannery wastewaters.

Future perspectives include the optimization of the ion-exchange, adjusting parameteres such as column height and elution flow rates, as well as the opportuinty of setting-up serial processses or modify the structure of the zeolite to improve its adsorption capacity. Additionally, research on the regeneration of the column and the associated costs of scaling-up the process will be crutial tasks for its viability at an industrial level.

Acknowledgments

The authors would like to thank the Universidad de Lima and Centro de Innovación

Productiva y Transferencia Tecnológica del Cuero, Calzado, Textil, Confecciones e Industrias Conexas (CITEcall)

REFERENCES

1. Abdulrazzaq, N.N., Al-sabbagh, B.H., Shanshool, H.A. 2021. Coupling of Electrocoagulation and microflotation for the removal of textile dyes from aqueous solutions, J. Water Proc. Eng. 40, 101906, https://doi.org/10.1016/j.jwpe.2020.101906.
2. Aboulhassan, M.A., El Ouarghi, H., Ait Benichou, S., Ait Boughrous, A., Khalil, F. 2018. Influence of experimental parameters in the treatment of tannery wastewater by electrocoagulation, Separation Science and Technology, 53:17, 2717-2726, doi: 10.1080/01496395.2018.1470642.
3. Aguilar-Ascón, E., Marrufo-Saldaña, L., Neyra-Ascón, W. 2019. Reduction of Total Chromium Levels from Raw Tannery Wastewater via Electrocoagulation using Response Surface Methodology. Journal of Ecological Engineering, 20(11), 217-224.https://doi.org/10.12911/22998993/113191.
4. Aguilar, E., Marrufo, L., Neyra, W. 2020. Efficency of electrocoagulation method to reduce COD, BOD and TSS in tannery industry wastewater: application of the box–behnken design. Leather and Footwear Journal. https://doi.org/10.24264/lfj.20.3.1.
5. Aguilar Ascon, E., Marrufo Saldaña, L., Neyra Ascón, W. 2023. Reducing Tannery Wastewater Pollutants through a Magnetic-Field and Ozone-Treatment Electrocoagulation System using Response Surface Methodology. Journal of Ecological Engineering, 25(1), 74-83. https://doi.org/10.12911/22998993/173566.
6. Asaithambi, P., Susree, M., Saravanathamizhan, R., M. Matheswaran, M. 2012. Ozone assisted electrocoagulation for the treatment of distillery ef fl uent. DES 297, 1e7. https://doi.org/10.1016/j.desal.04.011.
7. Asaithambi, P., Aziz, A.R.A. Daud, W.M.A.B.W. 2016. Integrated ozone-electrocoagulation process for the removal of pollutant from industrial effluent: optimization through response surface methodology. Chem. Eng. Process 105, 92–102. https://doi.org/10.1016/j.cep.2016.03.013.
8. Aziz, A.R.A., Asaithambi, P., Daud, W.M.A.B.W. 2016. Combination of electrocoagulation with advanced oxidation processes for the treatment of distillery industrial effluent, Process Saf. Environ. Protect. 99-227–235.
9. Barzegara, G., Wu, J., Ghanbari, F. 2019. Enhanced treatment of greywater using electrocoagulation/ozonation: investigation of process parameters, Proc. Safety Environ. Prot. 121 - 125–132. https://doi.org/10.1016/j.psep.2018.10.013.
10. Behin, J., Farhadian, N., Ahmadi, M., Parvizi, M. 2015. Ozone assisted electrocoagulation in a rectangular internal-loop airlift reactor: Application to decolorization of acid dye. Journal of water process engineering, 8, 171-178.
11. Bishwatma, B., Sudha, G. 2022. Electrocoagulation and electrooxidation technologies for pesticide removal from water or wastewater: A review, Chemosphere, Volume 302, 134709, ISSN 0045-6535, https://doi.org/10.1016/j.chemosphere.2022.134709.
12. Burns, S.E., Yiacoumi, S., Tsouris, C. 1997. Microbubble generation for environmental and industrial separations. In Separation and Purification Technology. (Vol. 11, Issue 3, pp. 221–232). Elsevier BV. doi: 10.1016/s1383-5866(97)00024-5.
13. Can, O.T., Kobya, M., Demirbas, E., Bayramoglu, M. 2006. Treatment of the textile wastewater by combined electrocoagulation. Chemosphere 62, 181e187. https://doi.org/10.1016/j.chemosphere.(2006).05.022.
14. Choi, A.E.S., Futalan, C.C.M., J.J. Yee, J.J. 2020. Fuzzy optimization for the removal of uranium from mine 1 water using batch electrocoagulation: A case study. Nuclear Energy and Technology, 52(7), 1471–1480. https://doi.org/10.1016/j.net.12.016.
15. Chung, Y.CH., Son, D.-H., Ahn, D.-H. 2000. Nitrogen and organics removal from industrial wastewater using natural zeolite media. Water Science and Technology. 42. 127-134. 10.2166/wst.0506.
16. De Magalhães, LF., da Silva, G.R., Peres, AEC., Kooh, MRR. 2022. Zeolite Application in Wastewater Treatment. Adsorption Science & Technology. doi:10.1155/2022/4544104.
17. Deveci, E.Ü., Akarsu, C., Gönen, Ç., Özay, Y.2019. Enhancing treatability of tannery wastewater by integrated process of electrocoagulation and fungal via using RSM in an economic perspective. Process. Biochem. 84, 124–133. http://dx.doi.org/10.1016/J.PROCBIO.2019.06.016.
18. Dil, E.A., Ghaedi, M., Asfaram, A., Mehrabi, F., Sadeghfar, F. 2019. Efficient adsorption of Azure B onto CNTs/Zn: ZnO@Ni2P-NCs from aqueous solution in the presence of ultrasound wave based on multivariate optimization. Journal of Industrial and Engineering Chemistry, 74, 55–62. https://doi.org/10.1016/j.jiec.12.050.
19. Dogruel, S., Genceli, E., Germirli Babuna, F., Orhon, D. 2004. Ozonation of Nonbiodegradable Organics in Tannery Wastewater. Journal of environmental science and health. Part A, Toxic/hazardous substances & environmental engineering. 39. 1705-15. 10.1081/ESE-120037871.
20. Ebba, M., Asaithambi, P., Alemayehu, E. 2022. Development of electrocoagulation process for wastewater treatment: optimization by response surface

methodology. Heliyon 8(5).

21. Eberle, S., Viktor, S., Hilmar, B., S. Stefan, S. 2023. Natural Zeolites for the Sorption of Ammonium: Breakthrough Curve Evaluation and Modeling Molecules 28, no. 4: 1614. https://doi.org/10.3390/molecules28041614.
22. Ehsan Jafari, M., Reza, M., Heike, B., Peter, K. 2023. Impact of operating parameters of electrocoagulation-flotation on the removal of turbidity from synthetic wastewater using aluminium electrodes, Minerals Engineering, Volume 193, (2023),108007, https://doi.org/10.1016/j.mineng.108007.
23. Espinoza-Quiñones, FR., Fornari, M.M.T., Modenes, A.N., Palacio, S.M., Trigueros, D.G.E., Borba, F.H., A.D. Kroumov, A.D. 2009. Electrocoagulation efficiency of the tannery effluent treatment using aluminum electrodes, Water Sci Technol, 60, 2173-2185. https://doi.org/10.2166/ wst.518.
24. Fashi, F., Ghaemi, A., Behroozi, A.H. 2021. Piperazine impregnation on Zeolite 13X as a novel adsorbent for CO2 capture: experimental and modeling, Chemical Engineering Communications, (2021). 208:8, 1104-1120. https://doi.org/10.1080/00986445.2020.1746657.
25. Ham, K., Kim, B., Choi, K.Y. 2018. Enhanced ammonium removal efficiency by ion exchange process of synthetic zeolite after Na^+ and heat pretreatment. Water Science and Technology. 78.10.2166/wst.420.
26. Houshyar, Z., Khoshfetrat, B., E. Fatehifar, E. 2012. Influence of ozonation process on characteristics of prealkalized tannery effluents. Chem. Eng. J. 191, 59–65.
27. Huang, J., Kankanamge, N.R., Chow, C., Welsh, D.T. Li, T., Teasdale, P.R. 2018. Removing ammonium from water and wastewater using cost-effective adsorbents: A review. Journal of environmental sciences (China), 63, 174–197. https://doi.org/10.1016/j.jes.(2018).09.009.
28. Howe, K.J., Hand, D.W., John, C., Crittenden, R. 2012. Rhodes Trussell, George Tchobanoglous. Principles of Water Treatment. John Wiley & Sons Inc, New Jersey.
29. Iaconi, CD., Lopez, A., Ramadorai, R., Pinto, ACD., Passino, R. 2002. Combined chemical and biological degradation of tannery wastewater by a periodic submerged filter (SBBR). Water Res 36:2205–2214. doi:10.1016/S0043-1354(01)00445-6.
30. Ibrahim, F.N.D., Daud, Z., Abdul Latiff, A.A., Ridzuan, M.B., Ahmad, Z., Awang, H., Marto, A. 2017. Ammoniacal Nitrogen and COD Removal Using Zeolite-Feldspar Mineral Composite Adsorbent. International Journal of Integrated Engineering, 8(3). Retrieved from (2017). https://penerbit.uthm.edu.my/ojs/index.php/ijie/article/view/1478.
31. Kamimoto, K., Hagio, T., Jung, YJ. 2020. Development of Synthetic Magnetic Zeolite Adsorbents and Application to Ammonium Ion Removal. KSCE J Civ Eng 24, 1395–1399. https://doi.org/10.1007/s12205-020-2185-5.
32. Khamidun, M.H., Fulazzaky, M.A., Mohamad, E.I., Gheethi, AI.A., Md Ali, U., Muda, K., Hadibarata, T., & Razi, M. 2020. Adsorption of ammonium from wastewater treatment plant effluents on to the zeolite; A plug-flow column, optimisation, dynamic and isotherms studies. International Journal of Environmental Analytical Chemistry. 102.10.1080/03067319.2020.1849659.
33. Khamidun, M., Ali Fulazzaky, M., Al-Gheethi, A., Ali, U. Md., Muda, K., Hadibarata, T., Mohammad Razi, M. 2022. Adsorption of ammonium from wastewater treatment plant effluents on to the zeolite; A plug-flow column, optimisation, dynamic and isotherms studies, International Journal of Environmental Analytical Chemistry. 102:19, 8445-8466, doi:10.1080/03067319.2020.1849659.
34. Kong, X., Wang, Y., Ma, L., Huang, G., Zhang, Z., Han, Z. 2020. Leaching Behaviors of Chromium (III) and Ammonium-Nitrogen from a Tannery Sludge in North China: Comparison of Batch and Column Investigations. International journal of environmental research and public health, 17(16), 6003. https://doi.org/10.3390/ijerph17166003.
35. Kongnoo, A., Tontisirin, S., Worathanakul, P., CH. Phalakornkule, CH. 2016. Surface characteristics and CO2 adsorption capacities of acid-activated zeolite 13X prepared from palm oil mill fly ash, Fuel, Volume 193, Pages 385-394, ISSN 0016-2361, https://doi.org/10.1016/j.fuel.2016.12.087.
36. Lanzetta, A., Papirio, S., Oliva, A., Cesaro, A., Pucci, L., Capasso, E.M., Esposito, G., Pirozzi, F. 2023. Ozonation Processes for Color Removal from Urban and Leather Tanning Wastewater. Water 2023, 15, 2362. https://doi.org/10.3390/w15132362
37. Leta, S., Assefa, F., Gumaelius, L., Dalhammar, G. 2005. Biological nitrogen and organic matter removal from tannery wastewater in pilot plant operations in Ethiopia. Applied microbiology and biotechnology. 66. 333-9.10.1007/s00253-004-1715-2.
38. Măicăneanu, A., Bedelean, H., Burcă, S., Stanca, M. 2011. Evaluation of Ammonium Removal Performances of Some Zeolitic Volcanic Tuffs from Transylvania, Romania, Separation Science and Technology, 46:10, 1621-1630, doi:10.1080/01496395.2011.561666.
39. Malakootian, M., Mansoorian, H.J., Moosazadeh, M. 2010. Performance evaluation of electrocoagulation process using iron-rod electrodes for removing hardness from drinking water, Desalination, Volume 255, Issues 1–3, Pages 67-71. https://doi.org/10.1016/j.desal.2010.01.015.
40. Manenti, D., Módenes, A., Soares, P., Espinoza-Quiñones, F., Boaventura, R., Bergamasco, R., Vilar, V. 2014. Assessment of a multistage system

based on electrocoagulation, solar photo-Fenton-vand biological oxidation processes for real textile wastewater treatment. Chemical Engineering Journal. 252. 120–130.10.1016/j.cej.04.096.

41. Ouyang, W., Songsheng, Z., Chongjun, W., Xiaohui, H., Riyi, C., Lianghui, Z., Zhaolin, W. 2021. Dynamic ammonia adsorption by FAU zeolites to below 0.1 ppm for hydrogen energy applications, International Journal of Hydrogen Energy, Volume 46, Issue 64, Pages 32559-32569, ISSN 0360-3199, https://doi.org/10.1016/j.ijhydene.2021.07.107.
42. Pan, M., Zhang, M., Zou, X., Zhao, X., Deng, T., Chen, T., Huang, X. 2019. The investigation into the adsorption removal of ammonium by natural and modified zeolites: kinetics, isotherms, and thermodynamics. Water SA, 45(4), 648-656. https://dx.doi.org/10.17159/wsa/2019.v45.i4.7546.
43. Pan, L., Zhang, A., Yongjun, L., Zhe, L., Xingshe, L., Lu, Y., Zhuangzhuang, Y. 2022. Adsorption Mechanism of High-Concentration Ammonium by Chinese Natural Zeolite with Experimental Optimization and Theoretical Computation. Water. 14. 2413. 10.3390/w14152413.
44. Prabhakaran, N., Patchai murugan, K., Jothieswari, M. et al. 2022. Tannery wastewater treatment process to minimize residual organics and generation of primary chemical sludge. Int. J. Environ. Sci. Technol. 19, 8857–8870 (2022). https://doi.org/10.1007/s13762-021-03634-2
45. Preethi, V., Kalyani, K.S.P. K., Iyappan, C., Srinivasakannan, C., Balasubramaniam, N. 2009. Vedaraman, Ozonation of tannery effluent for removal of cod and color, J. Hazard. Mater., v.166, p. 150–154.
46. Probst, J. Couperthwaite, S., Graeme, M., Kaparaju, P. 2022. Ammoniacal nitrogen removal and reuse: Process engineering design and technoeconomics of zeolite N synthesis. Journal of Environmental Chemical Engineering. https://doi.org/10.1016/j.jece.107942.
47. Rahmani, A.R., Mahvi, A.H., Mesdaghinia, A.R. 2004. Investigation of ammonia removal from polluted waters by Clinoptilolite zeolite. Int. J. Environ. Sci. Technol. 1, 125–133 (2004). https://doi.org/10.1007/BF03325825.
48. Sefatjoo, P., Alavi, M.R.A., Moghaddam, A.R. 2020. Mehrabadi, Evaluating electrocoagulation pretreatment prior to reverse osmosis system for simultaneous scaling and colloidal fouling mitigation: Application of RSM in performance and cost optimization. Journal of Water Process Engineering, 35, 101201. https://doi.org/10.1016/j.jwpe.101201.
49. Sundhararasu, E., Hanna, R., Teija Kangas, J.P., Ulla, L, and Sari, T. 2022. Column Adsorption Studies for the Removal of Ammonium Using Na-Zeolite-Based Geopolymers" Resources 11, no. 12: 119. https://doi.org/10.3390/resources11120119.
50. Srinivasan, S.V., Mary, G.P.S., Kalyanaraman, C. 2012. Combined advanced oxidation and biological treatment of tannery effluent. Clean Techn Environ Policy 14, 251–256. https://doi.org/10.1007/s10098-011-0393-x.
51. Sriram, B., Abhinav, K., Jyoti, K., Ruthviz, K., Jayaprakash, V. 2023. A state-of-the-art review of the electrocoagulation technology for wastewater treatment, Water Cycle, Volume 4 , Pages 26-36, ISSN 2666-4453, https://doi.org/10.1016/j.watcyc.2023.01.001.
52. Thushari, D., Wijesinghe, N., Kithsiri, B., Dassanayake Sven Sommer G., Guttila, Y., Jayasinghe P.J., Scales, CH. 2016. Deli, Ammonium removal from high-strength aqueous Solutions by Australian zeolite, Journal of Environmental Science and Health, Part A, 51:8, 614-625, (2016). doi: 10.1080/10934529.2016.1159861.
53. Varank, G., Erkan, H., Yazýcý, S., Demir, A., Engin, G. 2014. Electrocoagulation of tannery wastewater using monopolar electrodes: process optimization by response surface methodology, Int J Environ Res, 8, 165–180. http://dx.doi.org/10.22059/IJER.2014.706.
54. Vukojevi´c Medvidovi´c, N., Vrsalovi´c, L., Svilovi´c, S., Bobanovi´c, A. 2022. Electrocoagulation vs. Integrate Electrocoagulation-Natural Zeolite for Treatment of Biowaste Compost Leachate – Whether the Optimum Is Truly Optimal. Minerals. https://doi.org/10.3390/min12040442.
55. Wang, S., Y. Peng, Y. 2010. Natural zeolites as effective adsorbents in water and wastewater treatment. Chemical Engineering Journal, 156(1), 11–24. doi: 10.1016/j.cej.10.029.
56. Wang, C., Guo, H., Leng, S., Yu, J., Feng, K., Cao, L., Huang, J. 2020. Regulación de la hidrofilicidad/hidrofobicidad de las zeolitas de aluminosilicato: una revisión. Revisiones críticas en ciencias del estado sólido y de los materiales, (2020). 46(4), 330–348. https://doi.org/10.1080/10408436.2020.1819198.
57. Wen, D., Ho, Y.S., Tang, X. 2006. Comparative sorption kinetic studies of ammonium onto zeolite. Journal of hazardous materials, 133(1-3), 252–256. https://doi.org/10.1016/j.jhazmat.10.020.
58. Wijesinghe, T., Dassanayake, K., Scales, P., Chen, D. 2016. Mitigation of nitrogen losses with Australian zeolites during the anaerobic digestion of swine manure.
59. Wu, Z., Dong, J., Yao, Y.W., Yang, Y., F. Wei, F. 2021. Continuous flowing electrocoagulation reactor for efficient removal of azo dyes: Kinetic and isotherm studies of adsorption. Environ. Technol. Innov. 22.
60. Xu, C., Wang, J., Yang, T., Chen, X., Liu, X., Ding, X. 2015. Adsorption of uranium by amidoximated chitosan-grafted polyacrylonitrile, using Response Surface Methodology. Carbohydrate Polymers, 121, 79–85. https://doi.org/10.1016/j.carbpol.12.024.

61. Xuejun, G., Larry, Z., Xiaomei, Li., Hung-Suck, P. 2007. Removal of Ammonium from RO Permeate of Anaerobically Digested Wastewater by Natural Zeolite, Separation Science and Technology, 42:14, 3169-3185, doi:10.1080/01496390701514949.
62. Zaied, B.K., Rashid, M., Nasrullah, M., Zularisam, A.W., Pant, D., Singh, L. 2020. A comprehensive review on contaminants removal from pharmaceutical wastewater by electrocoagulation process, Sci. Total, Environ. 726, 138095, https://doi.org/10.1016/j.scitotenv.2020.138095.
63. Zhao, CH., Chen, W. 2019. A review for tannery wastewater treatment: some thoughts under stricter discharge requirements. Environmental Science and Pollution Research. 26.10.1007/s11356-019-05699-6.
64. Zheng, H., Han, L., Ma, H., Zheng, Y., Zhang, H., Liu, D., S.P. Liang, S.P. 2008. Adsorption characteristics of ammonium ion by zeolite 13X. Journal of hazardous materials, 158 2-3, 577-84. https://doi.org/10.1016/j.jhazmat.01.115.